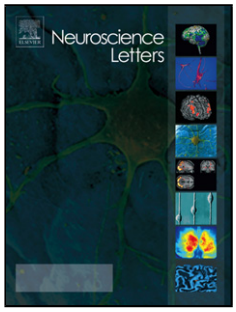

Title: *Atp13a2* expression in the periaqueductal gray is decreased in the *Pink1* -/- rat model of Parkinson disease

Author: Cynthia A. Kelm-Nelson Sharon A. Stevenson Michelle R. Ciucci

PII: S0304-3940(16)30208-7
DOI: http://dx.doi.org/doi:10.1016/j.neulet.2016.04.003
Reference: NSL 31953

To appear in: *Neuroscience Letters*

Received date: 9-10-2015
Revised date: 31-3-2016
Accepted date: 2-4-2016

Please cite this article as: Cynthia A.Kelm-Nelson, Sharon A.Stevenson, Michelle R.Ciucci, Atp13a2 expression in the periaqueductal gray is decreased in the Pink1 -/- rat model of Parkinson disease, Neuroscience Letters http://dx.doi.org/10.1016/j.neulet.2016.04.003

Atp13a2 expression in the periaqueductal gray is decreased in the *Pink1 -/-* rat model of Parkinson disease

Cynthia A. Kelm-Nelson [a], Sharon A. Stevenson [b], and Michelle R. Ciucci [a, c, d]

[a] Department of Surgery, Division of Otolaryngology
[b] Department of Zoology
[c] Neuroscience Training Program
[d] Department of Communication Sciences and Disorders
University of Wisconsin-Madison
Madison, WI USA

[*]Corresponding Author:
Cynthia A. Kelm-Nelson, Ph.D.
Department of Surgery, Division of Otolaryngology
1300 University Avenue, 483 Medical Sciences Center
University of Wisconsin-Madison
Madison, WI 53706 USA
Phone: 608-262-6122
Fax: 608-262-6356
Email: CAKelm@wisc.edu

Research Highlights:

- *Pink1* -/- rats do not show increased *alpha synuclein* gene expression.
- *Pink1* -/- rats do exhibit decreased *Atp13a2* expression in the periaqueductal gray.
- *Gad1* expression is reduced in the periaqueductal gray of *Pink1* -/- rats.

Abstract:

Vocal communication deficits are common in Parkinson disease (PD). Widespread alpha-synuclein pathology is a common link between familial and sporadic PD, and recent genetic rat models based on familial genetic links increase the opportunity to explore vocalization deficits and their associated neuropathologies. Specifically, the *Pink1* knockout (-/-) rat presents with early, progressive motor deficits, including

significant vocal deficits, at 8 months of age. Moreover, this rat model exhibits alpha-synuclein pathology compared to age-matched non-affected wildtype (WT) controls. Aggregations are specifically dense within the periaqueductal gray (PAG), a brainstem region involved in the coordination of emotional and volitional control of vocalizations. Here, we investigated changes in gene expression within the PAG at 8 months of age in *Pink1* -/- rats compared to WT. Our data demonstrate that *Pink1* -/- rat mRNA expression levels of alpha-synuclein are comparable to WT. However, *Pink1* -/- rats show significantly decreased levels of *Atp13a2*, a transmembrane lysosomal P5-type ATPase suggesting a potential mechanism for the observed abnormal aggregation. We found no difference in the expression of glucocerebrosidase (*Gba*) or the CASP8 and FADD-like apoptosis regulator (*Cflar*). Further, we show that mRNA expression levels of dopaminergic markers including *Th*, *D1* and *D2* receptor as well as GABA signaling markers including *Gaba-A* and glutamate decarboxylase 2 (*Gad2*) do not differ between genotypes. However, we found that glutamate decarboxylase 1 (*Gad1)* is significantly reduced in this PD model suggesting possible disruption of neurotransmission within the PAG. These results are the first to suggest the hypothesis that alpha-synuclein aggregation in this model is not a result of increased transcription, but rather a deficit in the breakdown and clearance, and that the observed vocal deficits may be related to impaired neural transmission. Altogether, these findings are consistent with the hypothesis that differences in neural substrate sensitivity contribute to the early pathogenesis of vocalizations and motivation to communicate in the *Pink1* -/- rat model of PD. Our results suggest novel therapeutic pathways, including the lysosomal

degradation pathway, which can be used in to further study the pathogenesis and treatment of vocal dysfunction PD.

Key Words:

Parkinson disease; rat; *Pink1*; periaqueductal gray; ultrasonic vocalization; alpha synuclein; *Atp13a2*; *Gad1*

1. Introduction:

Vocal deficits, including reduction in pitch and loudness, are common preclinical signs of Parkinson disease (PD). As the disease progresses, up to 90% of individuals have significant voice deficits that negatively impact quality of life and are difficult to treat [1-4]. Importantly, there is evidence that these changes in voice manifest prior to the onset of cardinal signs of the disease (resting tremor, bradykinesia and muscle rigidity) that are typically associated with significant striatal dopamine loss [5]. This suggests that voice dysfunction could be an early biomarker for PD diagnosis. However, the underlying neural pathology that contributes to vocal deficits in PD is poorly understood.

The discovery of genetic etiologies of PD has led to the creation of genetic rodent models that target genes known to cause PD [6, 7]. The *Pink1* knockout (-/-) rat expresses a genetic form of PD due to the complete knockout (loss of function) of the *Pink1* gene, which is related to the PARK6 phenotype of human familial PD [8, 9]. *Pink1* -/- models have early metabolic and mitochondrial degeneration including deficits in

mitochondrial respiration, morphology, and dynamics, as well as oxidative stress [10-15]. Most recently, characterization of the *Pink1* -/- rat has demonstrated aggregation of insoluble alpha synuclein (Asyn) in brainstem regions, including the periaqueductal gray (PAG) [16], as well as moderate dopaminergic cell loss in the substantia nigra [6]. Asyn aggregation is a key component of Lewy bodies [17-20] and although the exact degradation pathway is unknown, the autophagy-lysosomal pathway dysfunction has been implicated in the formation of aggregates and decreased Asyn turnover likely results in impaired protein clearance [21, 22].

The *Pink1* -/- rat model demonstrates motor impairment including significant impairment in ultrasonic vocalizations (USVs) [6, 16]. Specifically, at 8 months of age, *Pink1* -/- rats have significantly reduced intensity (loudness), bandwidth (frequency range) and peak frequency (upper range) of their 50-kHz frequency modulated (FM) calls as compared to non-affected wildtype (WT) controls. The brainstem PAG is responsible for vocal behavior across a wide range of vertebrate classes [23-25]. The PAG is responsive during the production of vocalizations and is hypothesized to be involved in the central organization of vocalizations as well as integration of motivational and emotional state [26]. Specifically, stimulation of the PAG elicits vocalizations [27], while lesions result in muteness [28, 29]. The PAG is also implicated in the coordination of vocalization [30],has numerous projections to lower brainstem regions that module vocal production (including nucleus ambiguus and retroambiguus)[31], as well as projections to the respiratory system and larynx [23, 32]. Specifically, microstimulation of cells adjacent to PAG results in excitation of laryngeal muscles in the macaque monkey [27] and vocal

fold control in squirrel monkey [33]. In addition, activation of the PAG has significant effects on neurotransmitter release, including dopaminergic [34, 35], and GABAergic signaling [36, 37] which suggests a role for multiple systems in vocal biology.

To assess mechanisms related to parkinsonian vocal deficits, we investigated relative gene expression changes in the PAG in the *Pink1* -/- rat model of PD and compared to aged-matched WT tissue. Using hypothesis-driven gene selection, we investigated changes in gene expression as a potential link to the observed reduction in acoustic properties and communication dysfunction in *Pink1* -/- rats. Specifically, we probed for: 1) significant increases in aggregation (*Asyn)* and apoptosis (CASP8 and FADD-like apoptosis regulator; *Cflar*), 2) reductions in lysosomal markers including ATPase type 13A2 (*Atp13a2*), glucocerebrosidase (*Gba*), 3) markers of dopamine including tyrosine hydroxylase (*Th*), dopamine receptor 1 and 2 (*D1,D2*), and 4) GABAergic neurotransmission including GABA-A receptor (*Gabrb2*) and glutamate decarboxylase 1 and 2 (*Gad1*, *Gad2*). As a control, we quantified mRNA expression levels for *Asyn*, *Atp13a2,* and *Gad1* in the striatum, a region that does not exhibit Asyn aggregation in this model [16].

2. Methods and Materials:

Animals

Long Evans rats (SAGE™ Research Labs, Boyertown, PA, USA [7]) were used for experimental analysis. Specifically, 11 *Pink1* -/- rats with a homozygous knockout of *Pink1* and 8 aged-matched WT Long Evans rat brains were used for

immunohistochemical analysis. An additional twelve male *Pink1* -/- and six WT rat brains were used for qPCR. The 8 month timepoint was selected for constitutive mRNA expression in the PAG at a defined early to middle disease stage [6, 16]. Animals were housed two per cage in standard polycarbonate cages with sawdust bedding on a reversed 12:12 hour light: dark cycle. All procedures were approved by the University of Wisconsin-Madison Animal Care and Use Committee (IACUC) and were conducted in accordance with the United States Public Health Service Guide for the Care and Use of Laboratory Animals.

Tissue collection, processing and quantification for Asyn immunohistochemistry

Rats were deeply anesthetized with 5% isoflurane, transcardially perfused with 200 ml of cold saline followed by 500mL of cold 4% paraformaldehyde in 0.1M phosphate buffer. Fixed brains were excised, post-fixed for 24 hr in 4% paraformaldehyde at 4 °C, cryoprotected in 0.02% sodium azide in 0.1M phosphate buffered saline solution and mounted on a freezing microtome where 60 micron coronal sections were harvested through the PAG. Free-floating brain sections were stored in glycerol cryoprotectant at -20 °C until they were stained for immunoreactivity. Staining is described in Grant et al. 2015; briefly, tissue was pretreated with proteinase K at 1:4000 (Invitrogen, Grand Island, NY) for 10 min [16]. Proteinase K treatment was used before the immunostaining to hydrolyze soluble proteins while retaining insoluble protein aggregations [38]. Sections were blocked in 20% normal goat serum and incubated overnight in primary solution: monoclonal rabbit anti-Asyn at 1:250 (04-1053, Millipore, Billerica, MA). Samples were incubated in conjugated biotinylated secondary solution at 1:500 for 90

min, incubated in an avidin biotin solution for 1 hr, visualized using filtered DAB with 0.02% hydrogen peroxide and coverslipped.

Two images from the dorsal medial and lateral PAG (DMPAG, LPAG) in each animal bilaterally were acquired using MetaMorph® at 20X magnification across 4-5 sections totaling 16-20 images per animal (at the approximate level of Bregma -5.40). Particle analysis was performed with a fixed inclusive threshold within a standardized rectangle box (0.43 mm x 0.28 mm), to include all aggregates as described in Grant et al. (2015) [39]. The area occupied was measured using MetaMorph®'s Total Pixel Area; measuring the area covered by the total number of computer-generated thresholded pixels.

Haematoxylin counterstaining and histology quantification

To investigate cell degeneration in the PAG, Asyn labeled tissue was counterstained with haematoxylin. Briefly, coverslips were removed, slices were quenched by rehydrating through alcohol dilutions, counterstained (SH30, Harris' Modified Haematoxylin with Acetic Acid, Fisher, Waltham, MA, USA), dehydrated and re-coverslipped.

Cells showing haematoxylin reactivity were quantified on a Nikon microscope with a Spot camera (Diagnostics Instruments, Inc.) and MetaMorph® software in a standardized box (315um x 409um) placed within the boundaries of PAG. The MetaMorph® autoscale function was used to calculate the correct exposure of the

image as a percent of the total range of light as a method to reduce variation in background between individual animals. Then, a computer-generated inclusive threshold was used to select labeled material; the threshold value for measurement inclusion was based on the grayscale values of the 8-bit photomicrograph. A single threshold was used across all animals. Using the Metamorph® Standard Area Count measure, the average of 6 sections containing PAG was used to generate an overall average count for each individual.

Tissue collection and processing for qPCR

At 8 months of age, animals were deeply anesthetized with isoflurane and rapidly decapitated. The brains were dissected out and immediately frozen and stored at -80°C. Brains were sliced in the coronal plane on a cryostat to a 250µm thickness at -15 °C and mounted on gelatin-coated glass slides. Specifically, 2mm tissue samples within the PAG (Bregma -7.8mm approximately, Figure 1A) and rostral striatum (Bregma 2.04, approximately) were micropunched using the Brain Punch Set (FST 18035-02, Foster City, CA, USA) under a dissection microscope over dry ice. For PAG, tissue from the left and right hemispheres was taken where the 4th ventricle and cerebral aqueduct were present; for rostral striatal tissue was taken where the genu of the corpus callosum and lateral ventricles were visible [40]. Anatomically equivalent sections of PAG and rostral striatum were used from each animal. Tissue samples were transferred to microcentrifuge tubes and stored at -80°C. For consistency, the same pair of researchers sliced and punched all of the study samples.

RNA extraction and reverse transcription

Sample order was randomized during processing. Tissue was homogenized with an electric Dremel tool, and total RNA was extracted with the Bio-Rad Aurum Total RNA Fatty and Fibrous Tissue Kit (Catalog No. 732-6830; Bio-Rd, Hercules, CA, USA) according to manufacturer's instructions. Total RNA was measured using a Nanodrop system (Thermo Scientific, Wilmington, DE, USA). Adjacent tissue micropunches were used to quantify the 28S:18S rRNA with an Agilent RNA 6000 Pico kit (Eukaryote Total RNA Pico, Agilent Technologies, Santa Clara, CA). Analysis of these data demonstrated satisfactory marker and ribosomal peaks as well as RNA concentrations and RNA Integrity Numbers (RIN; above 7.5).

DNase treated RNA (100ng/uL per cDNA reaction) was converted into single-stranded cDNA using the Invitrogen SuperScript III First-Strand Synthesis System (Catalog No. 18080-05; Invitrogen, Carlsbad, CA, USA).

Primer design and verification

NCBI Primer Blast was used to design primers for control reference genes (*Bactin* and *Gapdh*) and genes of interest (supplementary material) using the rat (*Rattus norvegius*) genome and based on hypothesis-driven selection. Reference genes were based on previous work in *Pink1* -/- models [6, 41]; our data demonstrate no difference in mean Ct values between genotypes for *Bactin* or *Gapdh*. Additionally, Netprimer (PREMIER Biosoft, Palo Alto, CA, USA) was used to examine secondary structure of all primers to avoid primer products. Non-template controls were run with each primer pair to check for formation of primer-dimers and non-specific amplification products. Specificity for

each primer pair was confirmed using melt curve analysis; all primer runs yielded single peak melt curves indicating amplification of single gene products. Furthermore, the qPCR reaction product for each gene was sequenced using Sanger sequencing with both forward and reverse primers at the University of Wisconsin Biotechnology Center to confirm that sequences match intended targets. Sequences are provided in the supplementary material Using NCBI BLAST all sequences were confirmed to match the intended targets.

Quantitative real-time PCR (qPCR)

Relative gene expression was determined for the PAG using real-time qPCR analysis following the MIQE guidelines for quantitative real-time PCR experiments [42]. All samples were prepared in reaction tubes containing the respective sample cDNA, nuclease-free water, characterized forward and reverse primers (5µM concentration, University of Wisconsin Biotechnology Center) and SsoFast EvaGreen Supermix (Catalog No. 172-5201). On each qPCR plate, five standards were run (1:10 serial dilutions, starting at 500ng/µL) with a Non Template negative control. Samples and standards were run in triplicate on each plate. Plates were read with the BioRad CFX96 Touch Real-Time PCR Detection System (Catalog No. 185-5195, Bio-Rad, Hercules, CA, USA). Briefly, each qPCR run entailed of an initiation step at 95°C for 30 sec, 40 cycles of 95°C for 5 sec, a 30 sec annealing phase, a 20 sec elongation phase at 72°C, and a melt curve from 60-88°C, 0.5 decrees for each 5 sec step. All plates were read following each elongation and melt curve stage.

Statistics

Immunohistochemical data was analyzed descriptively. Independent student's t-tests were used to analyze differences between genotypes for the haematoxylin counterstained tissue. For qPCR, data inclusion criteria consisted of run efficiencies between 90% and 110% as well as an R^2 of at least 0.990. The mean Ct value for each sample was defined as the average cycle number at which each sample triplicate crossed the amplification threshold, which was set a priori to 200 RFU. The mean Ct values for each sample were transformed via the Pfaffl Method to yield individual relative expression level values for each gene of interest for each rat [43]. All statistical analyses were conducted with SigmaPlot® 12.5 (Systat Software, Inc., San Jose, CA, USA). Data was rank transformed if it failed normality (Shapiro-Wilk test) and transformed data was used for subsequent statistical analysis. A Kruskal-Wallis One Way Analysis of Variance on Ranks with a Tukey test for multiple comparison procedures was used to compare mean Ct measures for each gene of interest between genotypes. The critical level for significance was set at 0.05 for rejecting the null hypothesis.

3. Results:

Asyn immunohistochemistry and haematoxylin counterstaining

Descriptively, there were clear differences in immunolabeling for Asyn positive aggregates between genotypes. WT animals did not demonstrate a high level of Asyn immunoreactivity; the *Pink1* -/- had increased pixel area immunolabeling (Figure 1B) in the PAG. For the counterstaining, there was no significant difference between

genotypes in average Standard Area Count within the PAG (t=0.631, df=13, *p*=0.54) (Figure 1C).

qPCR

The loss of the *Pink1* gene in the *Pink1* -/- rat was confirmed. There was a deletion of *Pink1* mRNA expression in the *Pink1* -/- rat compared to WT (H=10 (df=1), *p*=0.000079; Figure 1A). There was no significant difference in *Asyn* mRNA expression levels (F(1, 15)=0.043, *p*=0.84; Figure 2A). There was a significant difference in *Atp13a2* (F(1, 15)=14.79, *p*=0.002; Figure 2B); specifically the *Pink1* -/- rats had significantly reduced mRNA expression levels compared to WT. There were no significant differences in *Gba* (H=0.941 (df=1), *p*=0.33; Figure 2C) or *Cflar* (H=0.721 (df=1), *p*=0.40;data not displayed) mRNA expression levels.

There was a trend for a decrease in *D1* receptor mRNA expression (H=1.878 (df=1), *p*=0.08; Figure 2D). There were no significant differences in dopaminergic neurotransmission markers including *D2* receptor (F(1, 15)=0.17, *p*=0.69; data not displayed) or Th (H=0.40 (df=1), *p*=0.53; data not displayed) mRNA expression levels. Further, there were no differences in GABAergic markers including *Gabrb2* receptor (F(1, 15)=1.06, *p*=0.16; data not displayed) and *Gad2* (F(1, 15)=0.42, *p*=0.26; data not displayed) expression. However, there was a significant decrease in *Gad1* (F(1, 15)=2.99, *p*=0.05) mRNA expression in *Pink1* -/- compared to WT (Figure 2E).

Within the rostral striatum, there were no significant differences between genotypes for *Asyn* (F(1,16)=0.061, *p*=0.81), *Atp13a2* (F(1,16)=1.02, *p*=0.33), or *Gad1* (F(1,15)=1.48, *p*=0.24) (data not displayed).

4. Discussion:

In this study, we quantified mRNA transcription expression levels of genes within the PAG and rostral striatum of 8 mo old *Pink1* -/- and WT control animals. Past behavioral studies show robust vocalization deficits at this age in the *Pink1* -/- rat [16]. However, the neural mechanisms underlying these deficits are unknown. Anatomically, the PAG is connected with the nucleus retroambiguus and surrounding reticular formation and projects to motor neurons involved in vocal production [27, 30, 44]. Therefore, it is likely that neuropathology in the PAG may contribute to vocalization deficits in this model. We show that *Pink1* -/- rats have increased Asyn-positive immunolabeling compared to WT at this timepoint. However, our data demonstrate no significant difference in the relative mRNA expression of *Asyn* within the PAG. Moreover, we demonstrate a significant decrease in *Atp13a2* that suggests a possible mechanism for the observed aSyn aggregation, as *Atp13a2*, a lysosomal P-type transport ATPase, has been implicated in the pathogenesis of PD [45-48]. We did not observe differences in the lysosomal enzyme glucocerebrosidase (*Gba*) or apoptotic regulator *Cflar*. Furthermore, there was a significant decrease in *Gad1* expression levels, but not in *Gabrb2*, *Gad2* or the dopaminergic markers *Th* or *D2*. However, we did observe a trend for a decrease in the expression of *D1* receptor. Asyn aggregation has not been found in the striatum of

Pink1 -/- rats [16], and, in this study, we show that there are no differences in mRNA expression levels of *Asyn*, *Atp13A2*, and *Gad1*.

Pink1 -/- rats have reduced levels of Atp13a2

We show *Pink1* -/- rats have an approximate two fold decrease of *Atp13a2* mRNA expression. Impairment to the autophagy-lysosomal pathway and mutations in related genes, such as *Gba* and *Atp13a2*, have recently been linked to PD [46, 49, 50]. *Atp13a2* supports lysosomal and mitochondrial function by promoting the exosomal release of Asyn [49] and preventing parkinsonian-aSyn aggregation. Moreover, *Atp13a2* mutations are linked to autosomal recessive familial parkinsonism, and decreased expression of *Atp13a2* leads to significant PD-related mitochondrial dysfunction [51]. Mutations in *Atp13a2* in medaka fish lead to dopaminergic cell death [52] while overexpression of this gene protects against Asyn aggregations [49]. Additionally, cell cultures with reduced *Atp13a2* show lower levels of autophagy compared to normal cells. Interestingly, at this time point we do not see differences in relative gene expression of *Gba* or *Cflar* between *Pink1* -/- and WT. While links have been established between mutations in *Gba* and accumulation of proteins (Asyn) in PD, there is little evidence to suggest disruption of *Gba* in autosomal recessive PD. We did not analyze Gba enzyme activity/concentrations which would provide additional information at the protein level. Evidence suggests a role for apoptotic cell death in PD based on human post-mortem studies focusing on the nigrostriatal region [53]. Because neurodegeneration in the *Pink1* -/- rat mimics the slow progressive nature of PD, the rate of neuronal death maybe low at 8 months of age. It is possible that as

neurodegeneration advances rapidly with age in this model, apoptotic expression would significantly increase; similar to increases in apoptotic factors in the 6-OHDA rat infusion model [54] and mouse MPTP model [55] where cell death occurs at high rates. Thus, future work should target apoptotic markers at later biological time points.

aSyn accumulation and toxicity

In humans, Asyn is present in insoluble protein aggregates [56]. Several studies show that *Atp13a2* influences neuronal Asyn. For example, neuronal cultures lacking the *Atp13a2* gene demonstrate higher levels of Asyn compared to WT neurons [57]. Additionally, *Atp13a2* colocalizes with Asyn in Lewy bodies [58]. Recent immunohistochemical reports in the *Pink1* -/- model suggest that the levels of "Total Asyn" are comparable to WT [6]. Our data are consistent with these findings, as we report no difference in mRNA expression levels. However, our immunohistochemical observations are consistent with a previous study that report that *Pink1* -/- animals show proteinase-K resistant Asyn aggregations in the PAG suggesting that Asyn is not being broken down in this model [16]. The exact link between Asyn accumulation and cytotoxicity is unknown. Our results suggest aggregation may affect neurotransmission as well as behavioral output. Studies in transgenic mouse models (Thy-1 aSyn overexpression) have shown that Asyn pathology in the PAG co-occurs with significant and progressive vocalization deficits. Specifically, Thy-1 Asyn mice overexpress Asyn in the PAG [39]. There are multiple species of synuclein including fibrillary Asyn, phosphorylated Asyn, and soluble forms of Asyn as well as interacting proteins such as

synphilin-1; therefore, future work should target and confirm which forms are accumulating and potentially cytotoxic within this model.

Pink1 -/- rats show reduced mRNA expression levels of Gad1, but not other neurotransmitter-related genes

GABAergic dysfunction is implicated in neurological diseases and activity of glutamate decarboxylase (Gad), the rate-limiting synthesizing enzyme converting glutamate to GABA, is reduced in patients with PD [59, 60]. Interestingly, a decrease in plasma GABA levels is correlated with early-stage signs [61]. Within the basal ganglia, GABA activity is thought to influence the regulation of movement [62] and Gad gene therapy is suggested to be neuroprotective in nature [63]. Both isoforms Gad1 and Gad2 are expressed in the brain where GABA is used as a neurotransmitter. GABA neurons are found within the PAG in the rat [36], which then interconnect with other cell types in adjacent and projecting regions including the nucleus ambiguus. We report significant decreases in *Gad1* within the PAG in *Pink1* -/- animals, but not *Gad2*. Due to differences in their regional expression, activity, and localization, these results suggest a potential dysfunction in cytosolic GABA synthesis (*Gad1*) but not synaptosomal GABA release (*Gad2*) [64]. Decreases in GABA activity have been associated with disruption in vocal production. Of note, inhibition of GABAergic activity reduces rat and mouse pup vocalizations [65-67] and our findings may represent a pathway for vocalization disruption in the *Pink1* -/- rat. We found no difference in *Gabrb2* expression between genotypes; however, future experiments should examine additional GABAergic receptor subunit differences.

We found a slight trend for a reduction in *D1* receptor mRNA expression in the PAG of *Pink1* -/- rats. Past research suggests that the laryngeal sensorimotor system is sensitive to fine modulations of the dopaminergic system and manipulations of central dopamine lead to dramatic acoustic changes in rat vocalizations. For example, acoustic degradations, reductions in call rate, duration, intensity, bandwidth, and peak frequency, are influenced by D1 and D2 receptor antagonism with D1 antagonism altering parameters more so than D2 [68]. In this study, the 8 mo timepoint is considered early to mid-stage with only moderate dopamine loss [16]; thus, it is possible with the progression of the disease in this model that there would be a more substantial reduction in dopamine as degeneration progresses.

Pink1 -/- rats demonstrate deficits in social vocal communication. Specifically, a decrease in the average peak frequency of their ultrasonic vocalizations is robust at 8 mo of age [16]. The peak frequency measure has been implicated in affective communication in rodents [69]. The PAG is uniquely positioned to influence both the motor and affiliative aspects of vocal communication [24, 28, 30]. Here, we provide the first evidence that suggests that lysosomal dysfunction as well as disruption in the neural transmission in the PAG may represent an inability to effectively modulate socially-appropriate vocalizations, coordinate sensory inputs, and organize the appropriate physiological output. However, it is important to note that changes in mRNA do not constitute direct protein changes. Therefore, future studies should use protein validation methods to confirm pathology in this model. The neuroanatomical

composition of PAG is diverse in that it contains multiple types of neurons including dopamine, opioid, GABA, serotonin, and nitric oxide, among others [35, 36, 70-73]. Likewise, there are numerous efferent [74] and afferent [75] projections that traverse the PAG. However, it is interesting that our results are reflected on a tissue level, as micro tissue punches containing numerous cell types, which can then be inferred to a higher bio-behavioral level.

Future Directions and Broader Impacts

The characterization of the full rat genome provides the opportunity for disease-based research that can be integrated with behavioral findings. These data are the first to suggest a mechanistic role for the PAG in mediating vocalization deficits in this PD rat model. Our findings provide specific evidence for pathological biomarkers within the PAG as a target for future treatments. Although the underlying pathological mechanisms are not understood completely, deficits in vocalizations in this model are comparable to some voice deficits in humans with PD. Future research should investigate additional brain regions including the nucleus ambiguus, and peripheral structures such as the larynx, and correlate pathology (gene expression levels) to acoustic outputs. Moreover, a better characterization of resulting protein changes within the brain, for example using immunohistochemistry or western blotting for key proteins, is needed to demonstrate pathological morphology. To develop effective interventions for these parkinsonian vocal deficits, relationships between pathology and the consequences on vocal communication function must be thoroughly defined. A better understanding of the

neuropathology of PD, especially how it pertains to voice and speech deficits, will lead to optimized patient treatments.

Acknowledgments:

Funding sources: F32 DC014399 (Kelm-Nelson); R01 DC014358 (Ciucci); University of Wisconsin Department of Surgery-Division of Otolaryngology (Ciucci; Kelm-Nelson). We gratefully acknowledge Dr. Lauren Riters and Dr. Stephen Gammie for qPCR facilities, and John Szot for managerial support. We thank Caroline Angyal for data collection and assistance and Dr. Tiffany Glass and Katie Yang for manuscript revisions.

Financial Disclosure/Conflict of Interest: None

References:

[1] Marras, C., McDermott, M. P., Rochon, P. A., Tanner, C. M., Naglie, G., Lang, A. E. Predictors of deterioration in health-related quality of life in Parkinson's disease: Results from the DATATOP trial. Mov. Disord. 2008,23:653-9.

[2] Ho, A. K., Iansek, R., Marigliani, C., Bradshaw, J. L., Gates, S. Speech impairment in a large sample of patients with Parkinson's disease. Behav. Neurol. 1999,11:131-7.

[3] Hammer, M., Barlow, S. Laryngeal somatosensory deficits in Parkinson’s disease: implications for speech respiratory and phonatory control. Exp. Brain Res. 2010,201:401-9.

[4] Ciucci, M. R., Grant, L. M., Rajamanickam, E. S. P., Hilby, B. L., Blue, K. V., Jones, C. A., et al. Early Identification and Treatment of Communication and Swallowing Deficits in Parkinson Disease. Semin. Speech Lang. 2013,34:185-202.

[5] Stewart, C., Winfield, L., Hunt, A., Bressman, S. B., Fahn, S., Blitzer, A., et al. Speech dysfunction in early Parkinson's disease. Mov. Disord. 1995,10:562-5.

[6] Dave, K. D., De Silva, S., Sheth, N. P., Ramboz, S., Beck, M. J., Quang, C., et al. Phenotypic characterization of recessive gene knockout rat models of Parkinson's disease. Neurobiol. Dis. 2014,70:190-203.

[7] Baptista, M. A. S., Dave, K. D., Sheth, N. P., De Silva, S. N., Carlson, K. M., Aziz, Y. N., et al. A strategy for the generation, characterization and distribution of animal models by The Michael J. Fox Foundation for Parkinson’s Research. Dis. Model. Mech. 2013,6:1316-24.

[8] Kawajiri, S., Saiki, S., Sato, S., Hattori, N. Genetic mutations and functions of PINK1. Trends Pharmacol. Sci. 2011,32:573-80.
[9] Bonifati, V., Dekker, M. C. J., Vanacore, N., Fabbrini, G., Squitieri, F., Marconi, R., et al. Autosomal recessive early onset parkinsonism is linked to three loci: PARK2, PARK6, and PARK7. Neurol. Sci. 2002,23:s59-s60.
[10] Villeneuve, L., Purnell, P., Boska, M., Fox, H. Early Expression of Parkinson's Disease-Related Mitochondrial Abnormalities in PINK1 Knockout Rats. Mol. Neurobiol. 2014:1-16.
[11] Gautier, C. A., Kitada, T., Shen, J. Loss of PINK1 causes mitochondrial functional defects and increased sensitivity to oxidative stress. Proc. Natl. Acad. Sci. U. S. A. 2008,105:11364-9.
[12] Piccoli, C., Sardanelli, A., Scrima, R., Ripoli, M., Quarato, G., D'Aprile, A., et al. Mitochondrial respiratory dysfunction in familiar parkinsonism associated with PINK1 mutation. Neurochem. Res. 2008,33:2565-74.
[13] Yang, Y., Ouyang, Y., Yang, L., Beal, M. F., McQuibban, A., Vogel, H., et al. Pink1 regulates mitochondrial dynamics through interaction with the fission/fusion machinery. Proc. Natl. Acad. Sci. U. S. A. 2008,105:7070-5.
[14] Poole, A. C., Thomas, R. E., Andrews, L. A., McBride, H. M., Whitworth, A. J., Pallanck, L. J. The PINK1/Parkin pathway regulates mitochondrial morphology. Proc. Natl. Acad. Sci. U. S. A. 2008,105:1638-43.
[15] Deng, H., Dodson, M. W., Huang, H., Guo, M. The Parkinson's disease genes pink1 and parkin promote mitochondrial fission and/or inhibit fusion in Drosophila. Proc. Natl. Acad. Sci. U. S. A. 2008,105:14503-8.
[16] Grant, L. M., Kelm-Nelson, C. K., Hilby, B. L., Blue, K. V., Rajamanickam, E. S. P., Pultorak, J., et al. Evidence for early and progressive ultrasonic vocalization and oromotor deficits in a PINK1 knockout rat model of Parkinson disease. J. Neurosci. Res. 2015,In Press.
[17] Singleton, A. B., Farrer, M., Johnson, J., Singleton, A., Hague, S., Kachergus, J., et al. alpha-Synuclein locus triplication causes Parkinson's disease. Science. 2003,302:841.
[18] Hardy, J. Genetic analysis of pathways to Parkinson disease. Neuron. 2010,68:201-6.
[19] Chartier-Harlin, M. C., Kachergus, J., Roumier, C., Mouroux, V., Douay, X., Lincoln, S., et al. Alpha-synuclein locus duplication as a cause of familial Parkinson's disease. Lancet. 2004,364:1167-9.
[20] Ibanez, P., Bonnet, A. M., Debarges, B., Lohmann, E., Tison, F., Pollak, P., et al. Causal relation between alpha-synuclein gene duplication and familial Parkinson's disease. Lancet. 2004,364:1169-71.
[21] Mak, S. K., McCormack, A. L., Manning-Bog, A. B., Cuervo, A. M., Di Monte, D. A. Lysosomal degradation of alpha-synuclein in vivo. J. Biol. Chem. 2010,285:13621-9.
[22] Usenovic, M., Tresse, E., Mazzulli, J. R., Taylor, J. P., Krainc, D. Deficiency of ATP13A2 Leads to Lysosomal Dysfunction, α-Synuclein Accumulation, and Neurotoxicity. J. Neurosci. 2012,32:4240-6.
[23] Larson, C. R. The Midbrain Periaqueductal Gray: A Brainstem Structure Involved in Vocalization. J. Speech. Lang. Hear. Res. 1985,28:241-9.
[24] Jürgens, U. The Neural Control of Vocalization in Mammals: A Review. J. Voice. 2009,23:1-10.

[25] Gruber-Dujardin, E. Role of the periaqueductal gray in expressing vocalization. In: Brudzynski SM, ed. Handbook of Mammalian Vocalization: An Integrative Neuroscience Approach: Academic Press; 2010. p. 313-27.
[26] Jurgens, U. The role of the periaqueductal grey in vocal behaviour. Behav. Brain Res. 1994,62:107-17.
[27] Larson, C. R., Kistler, M. K. The relationship of periaqueductal gray neurons to vocalization and laryngeal EMG in the behaving monkey. Exp. Brain Res. 1986,63:596-606.
[28] Jurgens, U., Pratt, R. Role of the periaqueductal grey in vocal expression of emotion. Brain Res. 1979,167:367-78.
[29] Lindsley, D. B., Schreiner, L. H., Knowles, W. B., Magoun, H. W. Behavioral and EEG changes following chronic brain stem lesions in the cat. Electroencephalogr. Clin. Neurophysiol. 1950,2:483-98.
[30] Zhang, S. P., Davis, P. J., Bandler, R., Carrive, P. Brain stem integration of vocalization: role of the midbrain periaqueductal gray. J. Neurophysiol. 1994,72:1337-56.
[31] Ennis, M., Xu, S. J., Rizvi, T. A. Discrete subregions of the rat midbrain periaqueductal gray project to nucleus ambiguus and the periambigual region. Neuroscience. 1997,80:829-45.
[32] Yajima, Y., Hayashi, Y., Yoshi, N. The midbrain central gray substance as a highly sensitive neural structure for the production of ultrasonic vocalization in the rat. Brain Res. 1980,198:446-52.
[33] Jurgens, U., Zwirner, P. Individual hemispheric asymmetry in vocal fold control of the squirrel monkey. Behav. Brain Res. 2000,109:213-7.
[34] Heisler, E. K., Kittelberger, J. M. Both D1- and D2-like receptors Contribute to Dopamine-Induced Inhibition of Vocal Production in the Midbrain Periaqueductal Gray of a Teleost Fish. Front. Behav. Neurosci.
[35] Lu, J., Jhou, T. C., Saper, C. B. Identification of wake-active dopaminergic neurons in the ventral periaqueductal gray matter. J. Neurosci. 2006,26:193-202.
[36] Belin, M. F., Aguera, M., Tappaz, M., McRae-Degueurce, A., Bobillier, P., Pujol, J. F. GABA-accumulating neurons in the nucleus raphe dorsalis and periaqueductal gray in the rat: A biochemical and radioautographic study. Brain Res. 1979,170:279-97.
[37] Mugnaini, E., Oertel, W. H. An atlas of the distribution of GABAergic neurons and terminals in the rat CNS as revealed by GAD immunohistochemistry. In: Bjorklund A, Hokfelt T, eds. Handbook of Chemical Neuroanatomy, Vol. 4 GABA and Neuropeptides in the CNS, part I Amsterdam: Elsevier Science; 1985.
[38] Fernagut, P. O., Hutson, C. B., Fleming, S. M., Tetreaut, N. A., Salcedo, J., Masliah, E., et al. Behavioral and histopathological consequences of paraquat intoxication in mice: effects of alpha-synuclein over-expression. Synapse. 2007,61:991-1001.
[39] Grant, L. M., Richter, F. R., Miller, J. E., White, S. A., Fox, C. M., Zhu, C., et al. Vocalization deficits in mice over-expressing alpha-synuclein, a model of pre-manifest Parkinson's disease. Behav. Neurosci. 2014,128:110-21.
[40] Paxinos, G., Watson, G. The Rat Brain in Stereotaxic Coordinates. 5 ed. Burlington, MA: Elsevier; 2005.
[41] Gómez-Sánchez, R., Gegg, M. E., Bravo-San Pedro, J. M., Niso-Santano, M., Alvarez-Erviti, L., Pizarro-Estrella, E., et al. Mitochondrial impairment increases FL-PINK1 levels by calcium-dependent gene expression. Neurobiol. Dis. 2014,62:426-40.

[42] Bustin, S. A., Benes, V., Garson, J. A., Hellemans, J., Huggett, J., Kubista, M., et al. The MIQE guidelines: minimum information for publication of quantitative real-time PCR experiments. Clin. Chem. 2009,55:611-22.
[43] Pfaffl, M. W. A new mathematical model for relative quantification in real-time RT–PCR. Nucleic Acids Res. 2001,29:e45-e.
[44] Holstege, G. Anatomical study of the final common pathway for vocalization in the cat. J. Comp. Neurol. 1989,284:242-52.
[45] Vilariño-Güell, C., Soto, A. I., Lincoln, S. J., Yahmed, S. B., Kefi, M., Heckman, M. G., et al. ATP13A2 variability in Parkinson disease. Hum. Mutat. 2009,30:406-10.
[46] Dehay, B., Ramirez, A., Martinez-Vicente, M., Perier, C., Canron, M.-H., Doudnikoff, E., et al. Loss of P-type ATPase ATP13A2/PARK9 function induces general lysosomal deficiency and leads to Parkinson disease neurodegeneration. Proc Natl Acad Sci 2012,109:9611-6.
[47] Ramirez, A., Heimbach, A., Grundemann, J., Stiller, B., Hampshire, D., Cid, L. P., et al. Hereditary parkinsonism with dementia is caused by mutations in ATP13A2, encoding a lysosomal type 5 P-type ATPase. Nat. Genet. 2006,38:1184-91.
[48] Di Fonzo, A., Chien, H. F., Socal, M., Giraudo, S., Tassorelli, C., Iliceto, G., et al. ATP13A2 missense mutations in juvenile parkinsonism and young onset Parkinson disease. Neurology. 2007,68:1557-62.
[49] Kong, S. M. Y., Chan, B. K. K., Park, J.-S., Hill, K. J., Aitken, J. B., Cottle, L., et al. Parkinson's disease-linked human PARK9/ATP13A2 maintains zinc homeostasis and promotes α-Synuclein externalization via exosomes. Hum. Mol. Genet. 2014,23:2816-33.
[50] Kong, B., Yang, T., Gu, J. W., Kuang, Y. Q., Cheng, L., Yang, W. T., et al. The association between lysosomal protein glucocerebrosidase and Parkinson's disease. Eur. Rev. Med. Pharmacol. Sci. 2013,17:143-51.
[51] Park, J.-S., Koentjoro, B., Veivers, D., Mackay-Sim, A., Sue, C. M. Parkinson's disease-associated human ATP13A2 (PARK9) deficiency causes zinc dyshomeostasis and mitochondrial dysfunction. Hum. Mol. Genet. 2014,23:2802-15.
[52] Matsui, H., Sato, F., Sato, S., Koike, M., Taruno, Y., Saiki, S., et al. ATP13A2 deficiency induces a decrease in cathepsin D activity, fingerprint-like inclusion body formation, and selective degeneration of dopaminergic neurons. FEBS Lett. 2013,587:1316-25.
[53] Tatton, N. A., Maclean-Fraser, A., Tatton, W. G., Perl, D. P., Olanow, C. W. A fluorescent double-labeling method to detect and confirm apoptotic nuclei in Parkinson's disease. Ann. Neurol. 1998,44:S142-8.
[54] He, Y., Lee, T., Leong, S. K. 6-Hydroxydopamine induced apoptosis of dopaminergic cells in the rat substantia nigra. Brain Res. 2000,858:163-6.
[55] Novikova, L., Garris, B. L., Garris, D. R., Lau, Y. S. Early signs of neuronal apoptosis in the substantia nigra pars compacta of the progressive neurodegenerative mouse 1-methyl-4-phenyl-1,2,3,6-tetrahydropyridine/probenecid model of Parkinson's disease. Neuroscience. 2006,140:67-76.
[56] Spillantini, M. G., Schmidt, M. L., Lee, V. M.-Y., Trojanowski, J. Q., Jakes, R., Goedert, M. alpha-Synuclein in Lewy bodies. Nature. 1997,388:839-40.
[57] Usenovic, M., Tresse, E., Mazzulli, J. R., Taylor, J. P., Krainc, D. Deficiency of ATP13A2 leads to lysosomal dysfunction, alpha-synuclein accumulation, and neurotoxicity. J. Neurosci. 2012,32:4240-6.

[58] Murphy, K. E., Cottle, L., Gysbers, A. M., Cooper, A. A., Halliday, G. M. ATP13A2 (PARK9) protein levels are reduced in brain tissue of cases with Lewy bodies. Acta neuropathologica communications. 2013,1:11.
[59] Lanoue, A. C., Dumitriu, A., Myers, R. H., Soghomonian, J. J. Decreased glutamic acid decarboxylase mRNA expression in prefrontal cortex in Parkinson's disease. Exp. Neurol. 2010,226:207-17.
[60] Buchanan, R. J., Gjini, K., Darrow, D., Varga, G., Robinson, J. L., Nadasdy, Z. Glutamate and GABA concentration changes in the globus pallidus internus of Parkinson's patients during performance of implicit and declarative memory tasks: A report of two subjects. Neurosci. Lett. 2015,589:73-8.
[61] Tong, Q., Xu, Q. R., Xia, Q., Yuan, Y. S., Zhang, L., Sun, H. B., et al. Correlations between plasma levels of amino acids and nonmotor symptoms in Parkinson's disease. J. Neural Transm. 2015,122:411-7.
[62] Brown, P., Oliviero, A., Mazzone, P., Insola, A., Tonali, P., Di Lazzaro, V. Dopamine Dependency of Oscillations between Subthalamic Nucleus and Pallidum in Parkinson's Disease. The Journal of Neuroscience. 2001,21:1033-8.
[63] Luo, J., Kaplitt, M. G., Fitzsimons, H. L., Zuzga, D. S., Liu, Y., Oshinsky, M. L., et al. Subthalamic GAD gene therapy in a Parkinson's disease rat model. Science. 2002,298:425-9.
[64] Soghomonian, J. J., Martin, D. L. Two isoforms of glutamate decarboxylase: why? Trends Pharmacol. Sci. 1998,19:500-5.
[65] Takahashi, A., Yap, J., Bohager, D., Faccidomo, S., Clayton, T., Cook, J., et al. Glutamatergic and GABAergic modulations of ultrasonic vocalizations during maternal separation distress in mouse pups. Psychopharmacology (Berl.). 2009,204:61-71.
[66] Fish, E. W., Sekinda, M., Ferrari, P. F., Dirks, A., Miczek, K. A. Distress vocalizations in maternally separated mouse pups: modulation via 5-HT1A, 5-HT1B and GABAA receptors. Psychopharmacology (Berl.). 2000,149:277-85.
[67] Olivier, B., Molewijk, E., van Oorschot, R., van der Heyden, J., Ronken, E., Mos, J. Rat pup ultrasonic vocalization: effects of benzodiazepine receptor ligands. Eur. J. Pharmacol. 1998,358:117-28.
[68] Ringel, L. E., Basken, J. N., Grant, L. M., Ciucci, M. R. Dopamine D1 and D2 receptor antagonism effects on rat ultrasonic vocalizations. Behav. Brain Res. 2013,252:252-9.
[69] Willuhn, I., Tose, A., Wanat, M. J., Hart, A. S., Hollon, N. G., Phillips, P. E. M., et al. Phasic Dopamine Release in the Nucleus Accumbens in Response to Pro-Social 50 kHz Ultrasonic Vocalizations in Rats. J. Neurosci. 2014,34:10616-23.
[70] Jurgens, U., Lu, C. L. Interactions between glutamate, GABA, acetylcholine and histamine in the periaqueductal gray's control of vocalization in the squirrel monkey. Neurosci. Lett. 1993,152:5-8.
[71] Lovick, T. A., Key, B. J. Inhibitory effect of nitric oxide on neuronal activity in the periaqueductal grey matter of the rat. Exp. Brain Res. 1996,108:382-8.
[72] Clements, J. R., Beitz, A. J., Fletcher, T. F., Mullett, M. A. Immunocytochemical localization of serotonin in the rat periaqueductal gray: a quantitative light and electron microscopic study. J. Comp. Neurol. 1985,236:60-70.

[73] Gonzalez-Hernandez, T., Conde-Sendin, M., Meyer, G. Laminar distribution and morphology of NADPH-diaphorase containing neurons in the superior colliculus and underlying periaqueductal gray of the rat. Anat. Embryol. (Berl.). 1992,186:245-50.
[74] Hamilton, B. L., Skultety, F. M. Efferent connections of the periaqueductal gray matter in the cat. J. Comp. Neurol. 1970,139:105-14.
[75] Keay, K. A., Feil, K., Gordon, B. D., Herbert, H., Bandler, R. Spinal afferents to functionally distinct periaqueductal gray columns in the rat: An anterograde and retrograde tracing study. J. Comp. Neurol. 1997,385:207-29.

Figure Legends:

Figure 1. A. Location and sizes of periaqueductal gray (PAG) tissue samples collected for real-time qPCR. Representative Nissl stained brain section, 50um thick sections. Photomicrograph at 10X magnification. Circular holes (represented by dashed circle) were centered within the PAG and illustrate the location (approximately Bregma -7.80mm) and punch size (2mm diameter). Abbreviations: Aq (cerebral aqueduct), PAG (periaqueductal gray). Color contrast has been optimized using Adobe Photoshop CC (Version 6) to clarify anatomical landmarks. Graph indicates alpha-synuclein (*Asyn*) mRNA expression in WT (white bar, n=5) and *Pink1* -/- (black bar, n=12) PAG 2mm tissue punches. All data was analyzed with the Pfaffl Method, normalized to reference genes (*ßactin*, *Gapdh*) expression. Error bars are standard error of the mean. * indicates significant differences between genotypes (p<0.01). B. Alpha-synuclein (Asyn) immunohistochemistry. Average pixel area of aggregated Asyn immunolabeling in the PAG. Horizontal line indicates background-labeling threshold. Photomicrographs of Asyn immunohistochemistry, one WT and one *Pink1* -/- rat. C. Haematoxylin counterstaining in the PAG. Average standard area count of haematoxylin labeled cells in WT (white bar, n=7) and *Pink1* -/- (black bar, n=8) within the PAG. Representative Haematoxylin stained coronal brain sections (40um). All photomicrographs at 20X magnification, scale bar is 0.01mm.

Figure 2. qPCR analysis of PAG tissue. A. alpha-synuclein (*Asyn*) mRNA expression in WT (white bar, n=5) and *Pink1* -/- (black bar, n=12) PAG 2mm tissue punches. B. glucocerebrosidase (*Gba*) mRNA expression, C. ATPase type 13A2 (*Atp13a2*) gene expression D. D1 receptor gene expression (D1) and D. GAD1 (*Gad1*) mRNA

expression levels. All data was analyzed with the Pfaffl Method, normalized to reference genes (*ßactin*, *Gapdh*) expression. Error bars are standard error of the mean. ** indicates significant differences between genotypes ($p<0.01$); * represents p=0.05, # represents a trend, $p=0.08$.

Fig 1

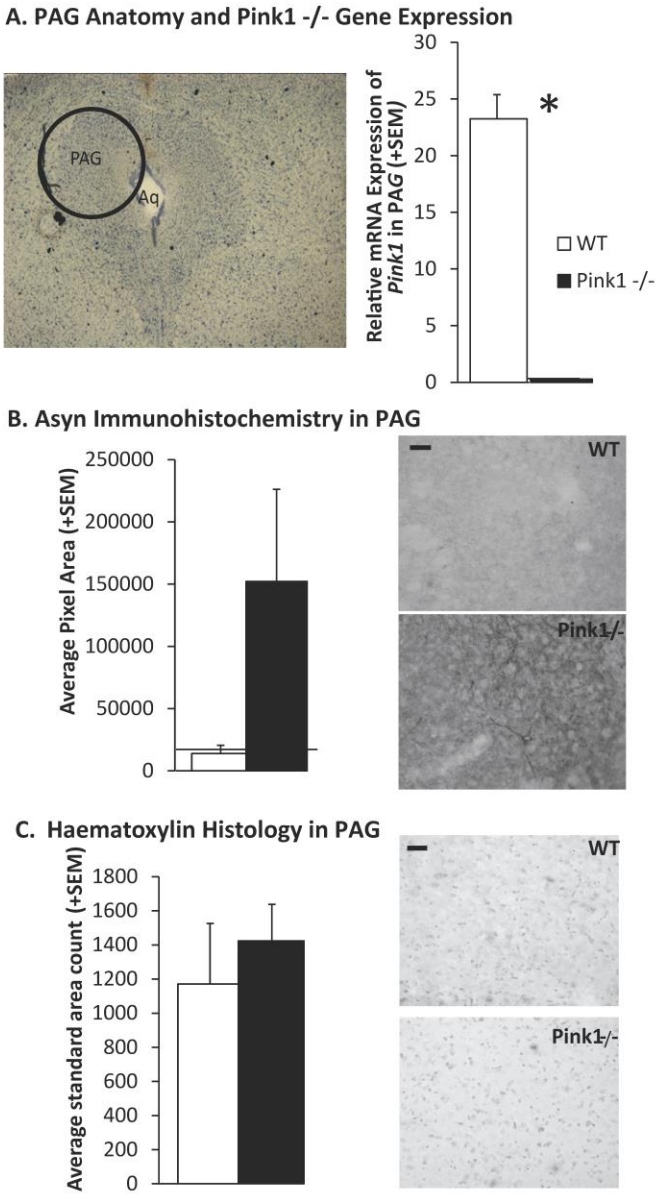

Fig 2